Decay of Ir^{196}†

W. N. BISHOP*
Brookhaven National Laboratory, Upton, New York
(Received 18 December 1964)

Iridium-196 (120 min) has been produced by the (d,α) reaction on Pt^{198}. The iridium was chemically separated from the target material. Gamma-ray, beta-ray, gamma-gamma, beta-gamma, and gamma-ray sum coincidence spectra were measured. Ir^{196} decays by a single beta group with an end-point energy of 0.95 MeV. The beta decay is followed by a cascade of six gamma rays of 100, 355, 389, 442, 518, and 646 keV. This decay is compatible with the known level scheme of Pt^{196}.

I. INTRODUCTION

THE only iridium nuclide which would be expected to have a half-life greater than a few minutes and which has not been characterized is Ir^{196}. Butement and Poe[1] assigned to Ir^{196} a 9.7-day activity which they produced by irradiating platinum with high-energy neutrons and with gamma rays. Gardner's[2] attempts to find Ir^{196} in platinum foils which had been bombarded with deuterons were unsuccessful; however, he was able to set an upper limit of 5 h for the half-life. Gardner also attributed the 9.7-day activity to Ir^{189}. The decay of Ir^{196} populates levels in Pt^{196}. These levels have been studied by (d,p) reactions[3] on Pt^{195} and through the decay[4,5] of Au^{196}.

In the present work Ir^{196} was produced through the reaction $Pt^{198}(d,\alpha)Ir^{196}$. This nuclide was shown to decay with a half-life of 2 h by a single beta group followed by a cascade of six gamma rays.

II. SOURCE PREPARATION

The Ir^{196} was produced by irradiation of platinum metal with 20-MeV deuterons from the Brookhaven 60-in. cyclotron. The targets for most of the bombardments were cut from commercial platinum foil of natural isotopic composition. Other targets were prepared by electrodeposition[6] of platinum enriched[7] in Pt^{198} onto copper foils. Spectrographic analysis of both natural and enriched platinum showed that both osmium and iridium were below the limits of detection, 0.01%.

It was necessary to separate the iridium from the large amounts of gold and platinum activities produced from the (d,xn) and (d,p) reactions, respectively. Some Na^{24} and Mg^{27}, which recoiled from the aluminum face plate of the cyclotron, were also found. The copper backing of the enriched platinum targets was a source of various zinc and copper activities. The separation procedure given below is a combination of the methods of Gardner[2] and of Busch, Prospero and Naumann.[8]

The platinum was dissolved in boiling aqua regia and carriers of iridium, gold, sodium, magnesium, zinc, and nickel were added. The solution was evaporated to dryness, taken up in 12N HCl, evaporated to dryness, and taken up in 3N HCl. Gold was removed by four ethyl-acetate extractions. Stannous chloride was added and platinum was extracted into ethyl acetate six times. The resulting aqueous solution was placed on an ion-exchange column of 1.5 cm^2 cross-sectional area filled to 12 cm with Dowex 1×8, 50–100 mesh topped with 12 cm of Dowex 50W×8, 50–100 mesh. Iridium was eluted with 9N HCl. Sufficient base was added to lower the acid concentration to about 1.5N, and the iridium was reduced to the elemental state with magnesium. The precipitate was collected on a glass fiber filter and thoroughly washed with water, 7N nitric acid, water, and acetone. This gave a disc-shaped counting sample, 2 cm in diameter. Samples prepared in this manner were very pure radiochemically, containing only Ir^{192}, Ir^{194}, and Ir^{196}.

III. GAMMA RAY SPECTROMETRY

The gamma-ray spectra were recorded on a 400-channel pulse-height analyzer using 7.6-cm×7.6-cm cylindrical NaI crystals. Aluminum absorbers were used to shield the gamma detectors from the high-energy beta rays of Ir^{194}. The source was centered on the detector axis at a distance of 9.0 cm.

Figure 1 shows the spectrum of the iridium fraction from a natural target. Curve A was recorded 80 min. after the end of bombardment and contains both Ir^{194} and Ir^{196}. Curve B was taken 24 h after end of bombardment and is due almost entirely to Ir^{194}. Ir^{192} is present in about 5% of the Ir^{194}. Curve C was obtained by subtracting spectrum B, corrected for the decay of Ir^{194}, from spectrum A and is the spectrum of Ir^{196}. Figure 2 shows the spectrum of the iridium fraction

† This work was performed under the auspices of the U. S. Atomic Energy Commission.
* Present address: Babcock & Wilcox Company, Lynchburg, Virginia.
[1] F. D. S. Butement and A. J. Poe, Phil. Mag. **45**, 31 (1954).
[2] D. G. Gardner and W. W. Meinke, Phys. Rev. **114**, 822 (1959).
[3] B. L. Cohen and R. E. Price, Phys. Rev. **118**, 1582 (1960).
[4] H. Ikegami, K. Sugiyama, T. Yamazaki, and M. Sakai, Nucl. Phys. **41**, 130 (1963).
[5] A. H. Wapstra, J. F. W. Jansen, P. F. A. Goudsmit, and J. Oberski, Nucl. Phys. **31**, 575 (1962).
[6] A. G. Gray, *Modern Electroplating* (John Wiley & Sons, Inc., New York, New York, 1953), p. 358.
[7] This material, consisting of 56.8% Pt^{198}, 26.7% Pt^{196}, 11.6% Pt^{195}, and 4.9% Pt^{194} was supplied by the Isotopes Division, Oak Ridge National Laboratory, Oak Ridge, Tenn.
[8] D. D. Busch, J. M. Prospero, and R. A. Naumann, Anal. Chem. **31**, 884 (1959).

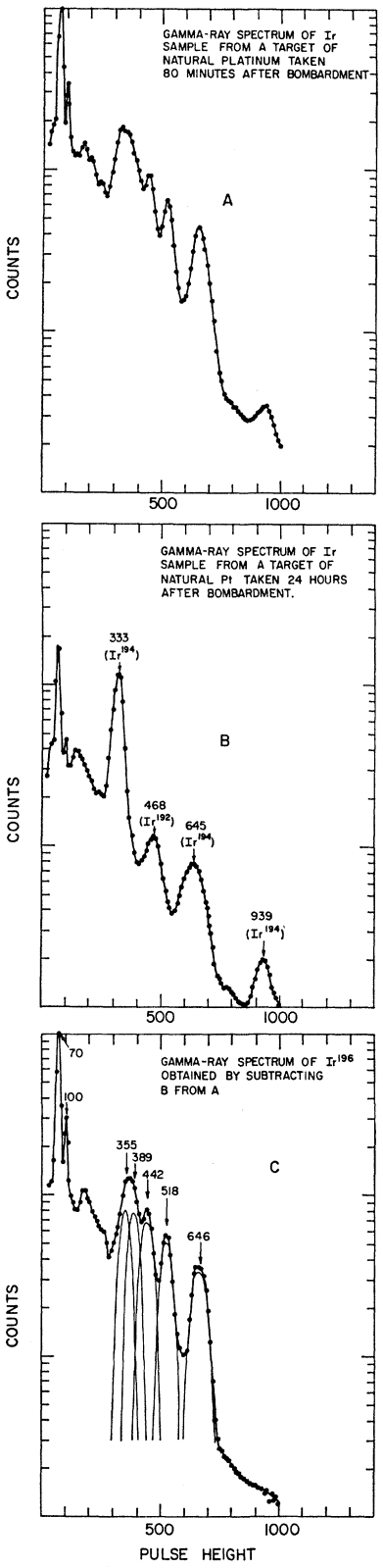

FIG. 1. Gamma-ray spectrum of Ir sample from a target of natural Pt. Curve A was taken 80 min after bombardment, curve B was taken 24 h after bombardment, and curve C was obtained by subtracting B, corrected for the decay of Ir^{194}, from A.

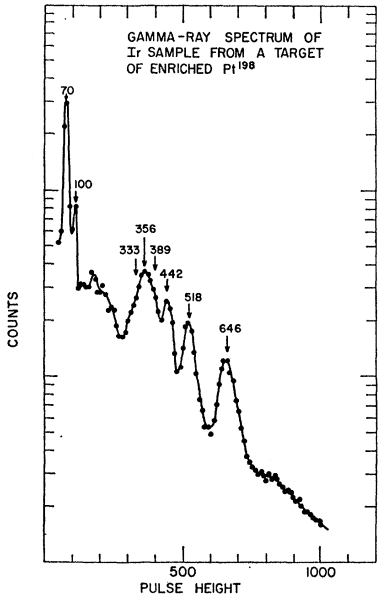

FIG. 2. Gamma-ray spectrum of Ir sample from a target of enriched Pt^{198}.

from an enriched platinum target. This curve was recorded 100 min after the end of bombardment and other than a 10% contribution due to Ir^{194} is identical to curve C of Fig. 1.

Spectral analysis was done by using Gaussian shapes for the full-energy peaks and by matching the Compton distributions with those of standards run under the same experimental conditions. The energies and intensities of the prominent gamma-ray peaks are listed in Table I. In the region of 300–700 keV the distribution is well accounted for. At lower energies the multiple subtractions produce errors of such magnitude that weak transitions could not be distinguished. After subtraction of the background and summing effects no gamma rays above 700 keV were found. Upper limits of 10% and 5% of the 646-keV transition were set for gamma rays between 100 and 300 keV and greater than 700 keV, respectively.

Five of the gamma rays are listed as being approximately equal in abundance. Comparison of gamma- and beta-ray intensities indicates that the absolute intensity of these gamma rays is approximately 100%. The low

TABLE I. Summary of Ir^{196} gamma-ray data.

Gamma-ray energy (keV)	Single-crystal intensity[b]	Coincidence quotient[a] with gamma rays of energy (keV)				
		370[c]	385	442	518	646
70	160±10	0.6	0.6	0.5	0.4	0.6
100	33± 5	0.3	0.3	0.3	0.3	0.4
355	102± 3	0.9	1.0	1.9	2.0	2.0
389	95± 3					
442	95± 3	0.9	1.0	···	1.0	1.0
518	98± 3	0.9	1.1	1.1	···	0.9
646	100	1.0	0.9	1.0	1.1	···

[a] The error index for the coincidence quotients is ±0.2.
[b] Relative to the 646-keV gamma ray as 100 units.
[c] See text for the explanation of window energy.

energy of the 100-keV photons and the high abundance of x rays indicate that this transition may be partially converted. If the transition occurs in 100% of the disintegrations the total conversion coefficient would have a value of 2.

For coincidence measurements a pair of crystals were placed at 90°, and an interdetector lead shield was used to reduce the effect of coincidences resulting from the scattering of photons between the crystals. Double-differential amplifiers were used with both detectors to allow the use of the zero cross-over point to derive timing signals for the fast inputs to a fast-slow coincidence system having a resolving time of 10^{-7} sec. The single-channel window was approximately 30 keV wide for each measurement.

The results of the gamma-gamma coincidence experiments, listed in Table I, are expressed as coincidence quotients q given by

$$q_{1,2}=(P_1 e^{\mu d}/D_2 C_w \epsilon_1)-\sum_i q_{1,i} D_i/D_2, \qquad (1)$$

where $q_{1,2}$ is the number of photons of γ_1, the gamma ray of interest, in coincidence with γ_2, divided by the number of photons of γ_2; P_1 is the coincident peak area of γ_1; $e^{\mu d}$ corrects for the fraction of γ_1 adsorbed by any material in its path; ϵ_1 is the peak efficiency, including the geometry factor, for the detection of γ_1; and C_w is the number of counts in the window of the single-channel analyzer. D_2 is the fraction of counts in the window due to γ_2, and knowing the window width, one can obtain this fraction from the single-crystal spectrum.

The term $\sum_i q_{1,i} D_i$ corrects for coincidences arising from "gating" events in the window due to γ_i, and $q_{1,i}$ is the relative number of γ_1 coincident with γ_i as determined from other coincidence experiments.

Spectra in coincidence with the 70- and 100-keV peaks were not recorded for several reasons. Both peaks ride on a large Compton distribution from higher energy transitions. Both peaks are quite sharp and the single channel could not be made sufficiently narrow to give a satisfactory peak to Compton ratio. The low energy of the transitions necessitates a high gain so that the pulses exceed the gating discriminator and the high gain causes appreciable noise in the amplifier. The 70-keV peak is due to both Ir^{196} and Ir^{194}.

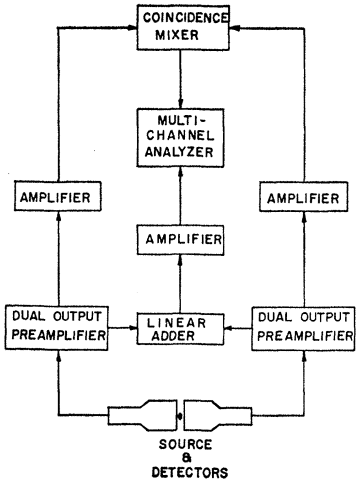

FIG. 3. Block diagram of the apparatus used to measure gamma-ray sum spectra.

The 355- and 389-keV transitions are not resolved as shown in Figs. 1 and 2. Due to the poor statistics in the coincidence spectra the decomposition of the composite peak is somewhat uncertain; thus the coincidence quotient for the composite 355- and 389-keV peak is given. Similarly the single-channel window cannot be set to contain the photopeak of only one of these gamma rays, particularly as care must be taken to exclude as much as possible the 328-keV photons of Ir^{194}. The window was centered at 370 keV for one spectrum and at 385 keV for another. Although appreciable amounts of both the 355- and 389-keV gamma rays were in each window, only small contributions of the 328-keV transition of Ir^{194} and the 442-keV photons of Ir^{196} were included.

Most of the coincidence experiments used targets of natural platinum as they were larger and thus gave higher disintegration rates. Other than the activity level, the coincidence spectra were the same from both natural and enriched targets.

The gamma-gamma coincidence studies indicate that each of the transitions is in coincidence with all of the others. This could be explained by a cascade of six gamma rays. In order to confirm this hypothesis the 4π gamma sum-coincidence spectrum was measured. The experimental arrangement is shown in Fig. 3. The sample was sandwiched between two 1.4 g/cm^2 copper discs and mounted between two 7.6-cm×7.6-cm NaI crystal assemblies with an interdetector distance of 0.3 cm. The gains of the two-detector assemblies were matched and their outputs were summed in the linear adder. The amplified sum pulses were fed to a pulse-height analyzer which was gated each time an event was detected in both crystals within the resolving time of the coincidence mixer.

The coincidence sum spectra are shown in Fig. 4. Curve A is the spectrum of both Ir^{194} and Ir^{196} and was recorded 80 min after the end of bombardment; curve B was taken 24 h after the end of bombardment and is due to only Ir^{194}; curve C is the Ir^{196} spectrum obtained by subtracting curve B, corrected for the decay of Ir^{194}, from curve A. The numerous peaks and shoulders in the spectra of Fig. 4 correspond to sums of the gamma rays of Ir^{194} or Ir^{196}, but the most interesting feature is the peak at 2.44 MeV in curve C. The sum of the energies of the six gamma rays of Ir^{196} is 2.45 MeV. If the 70-keV x ray is included instead of the 100-keV gamma ray, the sum is 2.42 MeV.

The sum-peak area can be measured in the sum-coincidence spectrum and can be calculated as the product of the disintegration rate and the product of the individual peak efficiencies plus the contribution of backscattered photons from one crystal into the other.

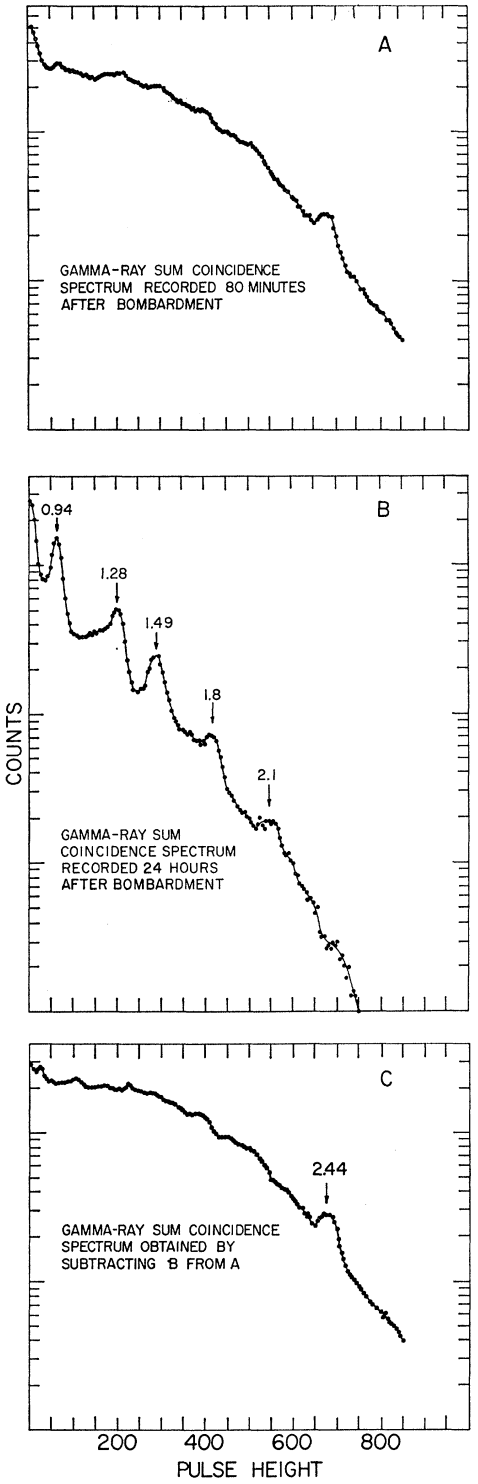

FIG. 4. Gamma-ray sum coincidence spectrum. Curve A was recorded 80 min after bombardment, curve B was recorded 24 h after bombardment, and C was obtained by subtracting B, corrected for the decay of Ir^{194}, from A.

The backscatter effect was considered sufficiently small to be ignored. The peak efficiencies were determined from the total gamma efficiencies and peak-to-total ratios given by Heath.[9] These values, corrected for attenuation in the copper absorbers, and the photopeak areas from the single-crystal spectrum were used to determine the disintegration rate. The measured sum-peak intensity is 422 counts/min compared with the calculated value of 394 counts/min. The 100-keV photons are shown to be of low relative abundance and this is attributed to partial internal conversion of this transition. This does not appreciably affect the sum peak calculation as the x ray[10] accompanying internal conversion would give a sum peak with essentially the same energy as would the 100-keV gamma ray.

IV. BETA-RAY SPECTROMETRY

The beta spectra were recorded using either a Pilot B scintillator or an anthracene crystal. The electronic system was the same as that used for gamma-ray spectrometry.

The beta spectrum of the iridium fraction from a natural platinum target is shown in Fig. 5, where curve A was recorded 90 min after end of bombardment and curve B was recorded 24 h after end of bombardment. The determination of the end point of the Ir^{196} beta rays is complicated by the large amount of Ir^{194} present. To circumvent this problem the spectrum of curve B was corrected for the decay of Ir^{194} and subtracted from that of curve A. The Fermi plot of the resulting Ir^{196} spectrum is shown as curve C of Fig. 5. The Fermi plot of

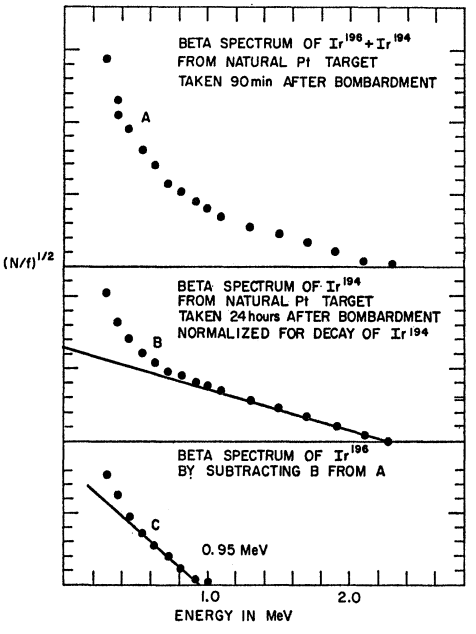

FIG. 5. Beta spectrum of Ir^{196} and Ir^{194} from a natural platinum target. Curve A was recorded 90 min after bombardment. Curve B was recorded 24 h after bombardment and has been corrected for the decay of Ir^{194}. Curve C was obtained by subtracting B from A.

[9] R. L. Heath, *Scintillation Spectrometry Gamma Ray Spectrum Catalogue* (Office of Technical Services, U. S. Department of Commerce, Washington, D. C.), IDO-16880-1.

[10] The fluorescence yield for K x rays in Pt is 0.94. C. D. Broyles, D. A. Thomas, S. K. Haynes, Phys. Rev. 89, 715 (1953).

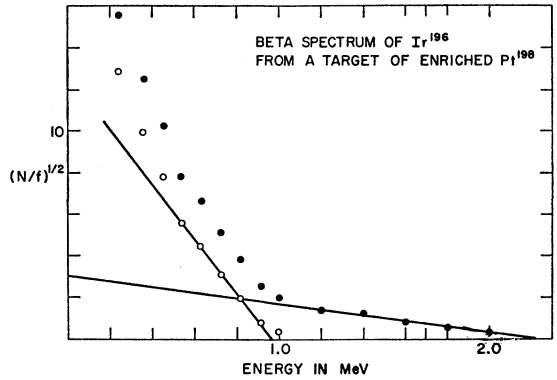

FIG. 6. Beta spectrum of Ir^{196} from a target of enriched Pt^{198}.

the beta spectrum of a sample from a target enriched in Pt^{198}, illustrated in Fig. 6, contains a much smaller contribution from Ir^{194}. The Ir^{196} beta spectra showed end points ranging from 0.93 to 0.98 MeV with a best value of 0.95±0.02 MeV. Below 500 keV the experimental points deviate from the straight line drawn through the higher energy points. This was shown to be due to scattering from the crystal.

Beta-gamma coincidence spectra were recorded gating with the same single-channel windows as in the gamma-gamma coincidence measurements. Samples from targets of natural and of enriched platinum were used. In each case the spectrum was identical to the singles beta spectrum, a single beta group with an end point of 0.95 MeV.

V. HALF-LIFE

The half-life of Ir^{196} was determined by the counting of total gamma rays, total beta rays, beta rays between 100- and 700-keV, gamma rays in the single-channel windows used in the coincidence measurements, and the 2.44-MeV gamma-ray sum peak. The decay curves were resolved into a long-lived component, presumably Ir^{192}, 19-h Ir^{194}, and Ir^{196}. The half-life of Ir^{196} was found to be 120±2 min.

VI. DISCUSSION

The results given above indicate that Ir^{196} decays by a single beta group followed by a cascade of six gamma rays. The total decay energy of 3.40 MeV is in good agreement with the predicted value of 3.44 MeV.[11] The most probable explanation for six gamma rays in cascade with no crossover transitions is that the spin of the levels increases with an increasing level energy. The level scheme for Pt^{196}, given in Fig. 7, includes results of this work and the level scheme of Ikegami *et al.*[4] The heavy lines are transitions from the decay of Ir^{196}, while the lighter lines, intensities, and energies are from the data of Ikegami for Au^{196} decay.

The 355-keV gamma ray is undoubtedly the transition from the first 2+ level to the ground state. The 518-keV gamma ray can be assigned to the transition from the 874-keV 4+ level. This is more probable than feeding the 355-keV level by a 646-keV gamma ray from the 1002-keV 3+ state since the 312-keV gamma ray, which would also depopulate this level, was not found.

It is now possible to feed the 874-keV level with the 446-keV gamma ray from the 1316-keV state, although this is subject to some objection as both Ikegami[4] and Wapstra[5] show higher energy transitions from the 1316-keV level, and these gamma rays were not detected in this work. Alternatively, the 874-keV level may be fed by a 646-keV gamma ray from a 1520-keV state having a spin of 6+. A 1520-keV level as well as the other expected levels of higher energies cannot be populated by the decay of Au^{196}. The (d,p) and (d,d') work of Mukharjee[12] also would probably not excite these levels due to their high spin state.

By choosing values for the adjustable parameters of

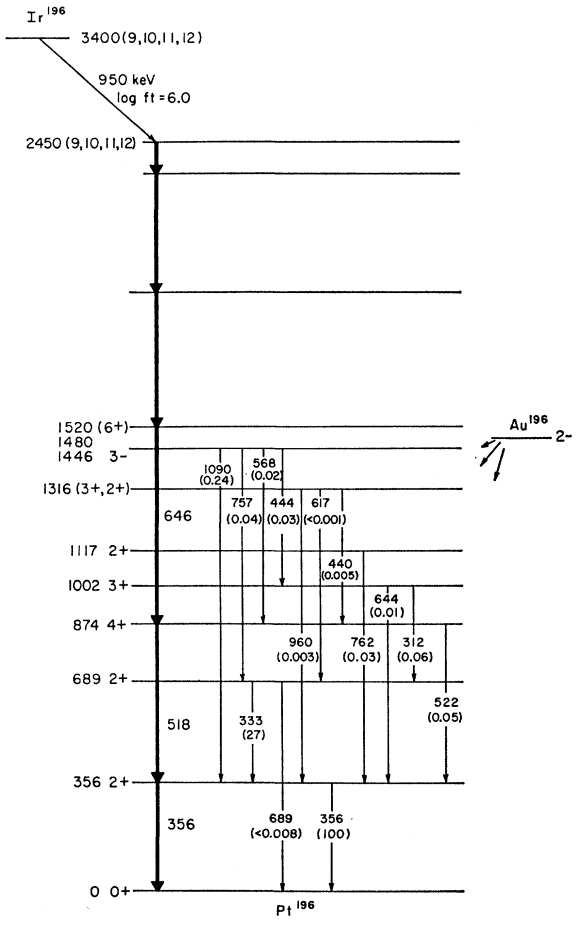

FIG. 7. Decay scheme of Ir^{196}. The heavy lines are transitions in the decay of Ir^{196}. The light lines are transitions in the decay of Au^{196} and are taken from Ref. 4.

[11] M. Hillman, Brookhaven National Laboratory Report No. BNL-846 (unpublished).

[12] P. Mukharjee, Nucl. Phys. (to be published).

the various nuclear models so that the low-lying states are well fitted, it is possible to calculate the energies of some of the higher levels. The 355-, 689-, 874-, and 1002-keV levels were used to determine the parameters for each model. The asymmetric rotor model of Davydov and Filippov[13] does not give a consistent set of parameters; however, when a first-order rotational-vibrational interaction[14] is included, an adequate fit for the four levels is obtained. The general asymmetric rotor model of Mallmann[15] and the nonadiabatic rotor model of Davydov and Chaban[16] are similar and give similar results. The calculated energies are given in Table II.

The calculations give weight to assigning the 646-keV gamma ray to the transition between the 1520- and 874-keV levels. In order to use calculated energies to place the remaining gamma rays in a level scheme, the calculations must be accurate to a few percent. This is the magnitude of the errors for the known levels and thus the calculated energies for higher states are not expected to have the necessary accuracy. The conversion coefficient of approximately 2 for the 100-keV transition is consistent with an $E2$ assignment.

A level can be placed at 2.45 MeV which probably has a spin of 9 to 12. This is the level of Pt^{196} which is populated in the beta decay of Ir^{196}. The logft value of 6.0 indicates that the beta decay must be either allowed or first forbidden, and that the level of Ir^{196} which is depopulated must also be a high-spin state.

The ground-state character of odd-odd nuclei frequently can be predicted by applying the coupling rules proposed by Gallagher and Moszkowski[17] to the Nilsson orbitals[18] assigned to the odd proton and neutron. The odd mass Ir nuclei are $\frac{3}{2}+[402\downarrow]$ in character and based on the ground state spins of the isotones of Ir^{196}, the odd neutron would be either $\frac{3}{2}-[512\downarrow]$, $\frac{5}{2}-[503\downarrow]$, or $\frac{1}{2}-[510\uparrow]$, which would give a ground state spin of 3-, 4-, or 1-.

Although Scharff-Goldhaber, Takahashi, and McKeown[19] have shown that the ground state spins of the other odd-odd Ir nuclei, with the exception of Ir^{194}, cannot be explained in this manner, it is still questionable to assign a spin of 9 to 12 to the ground state of Ir^{196} as no other Ir nuclide has such a high ground-state spin, and only Ir^{186} has a ground-state spin greater than 4.

Relatively low-lying levels of high spins are not uncommon in Ir nuclei, cf. Ir^{192} and Ir^{190}. A decay scheme which would fit the data for Ir^{196} might be very similar to that of Ir^{190m} (3 h)[20]; although the isomeric level of Ir^{196} could be much lower in energy and still populate high-spin states in Pt^{196}.

It is interesting to note that several workers[1,21] have found a 2.3 h iridium activity which was assigned to Ir^{195}. The beta-ray energy as well as some of the gamma rays reported by these authors agree with this work, and it is felt that their activity, which was assigned to Ir^{195}, was in fact Ir^{196}. Claflin, White, and Pool[22] have characterized Ir^{195} and have shown it to have none of the properties of the 2.3 h activity.

TABLE II. Comparison of calculated and experimental values for some energy levels of Pt^{196}. The energies are in keV. Square brackets indicate the percentage differences from the experimental values. The values of the parameters for each model are given.

Ik	Experimental energy[a]	Perturbed Davydov-Fillipov[b]	Davydov-Chaban[c]	Mallmann[d]
20	356	358[0.6]	355[0.3]	355[0.3]
22	689	689[0.0]	689[0.0]	688[0.1]
32	1002	991[1.1]	1023[2.1]	991[1.1]
40	878	884[0.7]	874[0.5]	879[0.1]
60	···	1514	1535	1495
		$\gamma=30°$	$\gamma=30°$	$A/C=4.2$
		$b=1.0\times10^{-4}$	$\mu=0.28°$	$k=0.9$
				$hc=30.1$
				$b=9.8\times10^{-4}$

[a] The experimental energy values are those of Ikegami *et al.* (Reference 4).
[b] Reference 14.
[c] Reference 16.
[d] Reference 15.

ACKNOWLEDGMENTS

The author would like to express his thanks to Dr. C. P. Baker and the staff of the Brookhaven cyclotron for technical advice and many bombardments, J. R. Holder for assistance with data processing, Dr. G. T. Emery, Dr. M. Hillman, Dr. B. M. Gordon, and Dr. R. L. Kiefer for helpful criticism of the manuscript, and Dr. P. Mukharjee for furnishing his results before publication.

[13] A. S. Davydov and G. F. Fillipov, Nucl. Phys. **8**, 237 (1958).
[14] C. A. Mallmann and A. K. Kerman, Nucl. Phys. **16**, 105 (1960).
[15] C. A. Mallmann, Nucl. Phys. **24**, 535 (1961).
[16] A. S. Davydov and A. A. Chaban, Nucl. Phys. **20**, 499 (1960).
[17] C. J. Gallagher, Jr., and S. A. Moszkowski, Phys. Rev. **111**, 1282 (1958).
[18] B. R. Mottelson and S. G. Nilsson, Kgl. Danske Videnskab. Selskab, Mat. Fys. Skrifter **1**, No. 8 (1959).
[19] G. Scharff-Goldhaber, K. Takahashi, and M. McKeown, in Proceedings of the International Congress of Nuclear Physics, Paris, July 1964 (unpublished).
[20] *Nuclear Data Sheets*, compiled by K. Way *et al.* (Printing and Publishing Office, National Academy of Sciences—National Research Council, Washington 25, D. C.).
[21] D. Christian, R. F. Mitchell, and D. S. Martin, Jr., Phys. Rev. **86**, 946 (1952). S. Homma and T. Kuroyanagi, J. Phys. Soc. Japan **16**, 841 (1961).
[22] A. B. Claflin, R. T. White, and M. L. Pool, Nucl. Phys. **36**, 652 (1962).